Materials Science and Engineering C 33 (2013) 1907–1913

Contents lists available at SciVerse ScienceDirect

Materials Science and Engineering C

journal homepage: www.elsevier.com/locate/msec

Fabrication of graphene–platinum nanocomposite for the direct electrochemistry and electrocatalysis of myoglobin

Wei Sun [a,b,*], Linfang Li [b], Bingxin Lei [a], Tongtong Li [b], Xiaomei Ju [b], Xiuzheng Wang [b], Guangjiu Li [b], Zhenfan Sun [a]

[a] College of Chemistry and Chemical Engineering, Hainan Normal University, Haikou 571158, PR China
[b] College of Chemistry and Molecular Engineering, Qingdao University of Science and Technology, Qingdao 266042, PR China

ARTICLE INFO

Article history:
Received 31 May 2012
Received in revised form 13 December 2012
Accepted 22 December 2012
Available online 2 January 2013

Keywords:
Myoglobin
Graphene
Pt nanoparticle
Electrochemical biosensor
Direct electrochemistry

ABSTRACT

In this paper a platinum (Pt) nanoparticle decorated graphene (GR) nanosheet was synthesized and used for the investigation on direct electrochemistry of myoglobin (Mb). By integrating GR–Pt nanocomposite with Mb on the surface of carbon ionic liquid electrode (CILE), a new electrochemical biosensor was fabricated. UV-Vis absorption and FT-IR spectra indicated that Mb remained its native structure in the nanocomposite film. Electrochemical behaviors of Nafion/Mb–GR–Pt/CILE were investigated with a pair of well-defined redox peak appeared, which indicated that direct electron transfer of Mb was realized on the underlying electrode with the usage of the GR–Pt nanocomposite. The fabricated electrode showed good electrocatalytic activity to the reduction of trichloroacetic acid in the linear range from 0.9 to 9.0 mmol/L with the detection limit as 0.32 mmol/L (3σ), which showed potential application for fabricating novel electrochemical biosensors and bioelectronic devices.

1. Introduction

There has been increasing interests in studying the direct electrochemistry of redox proteins, which can establish a desirable model for fundamental studies on the redox mechanism of the proteins in biological systems [1], and the results may be used to elucidate the relationship between their structures and biological functions. Meanwhile, studies on direct electron exchange between proteins and underlying electrodes can also provide a platform for fabricating biosensors, enzymatic bioreactors and biomedical devices [2]. Different kinds of protein film modified electrodes have been devised to achieve the direct electron transfer of redox proteins with the working electrodes, and the film can provide a favorable microenvironment for keeping the molecular structure and biocatalytic ability of the proteins [3,4]. In general proteins can retain their native structures and remain their biocatalytic ability in the films under the selected conditions. The immobilized proteins on the modified electrodes often exhibit fast electron transfer rate with a pair of well-defined redox peaks from active center of protein appeared. For example, Ding et al. studied direct electrochemical response of myoglobin (Mb) on the plane graphite electrode with 1-(2-hydroxyethyl)-3-methylimidazolium tetrafluoroborate as supporting electrolyte [5]. Ma et al. studied the direct electrochemistry and electrocatalysis of hemoglobin (Hb) with hyaluronic acid film on the edge-plane pyrolytic graphite electrode [6]. Sun et al. studied the electrochemical Mb biosensor on the electrodeposited Co nanoparticles decorated electrode [7].

As a new class of carbon material, graphene (GR) has attracted increasing attentions in different fields such as biosensor and nanodevices in recent years [8,9]. GR is a monolayer of sp^2 hybridized carbon atoms packed into a dense honeycomb crystal structure [10], which exhibits many unique characteristics such as high surface area, excellent electrical conductivity and electron mobility at room temperature, robust mechanical properties and flexibility [11]. In the meantime, the special properties of GR may provide insight to fabricate novel biosensors for virtual applications. The large surface area can increase the surface loading amount of the target enzyme molecules, and the excellent conductivity and small band gap are favorable for conducting electrons from the biomolecules [12]. GR-based chemical sensors also exhibit a much higher sensitivity because of the low electronic noise from thermal effect [13]. It has been reported that the integration of GR with metal nanoparticles can offer synergistic effects in electrocatalytic application. The GR-metal nanocomposites exhibit enhanced electronic and catalytic activity, which can be used for the construction of the electrochemical sensors with better performances. By decorating metal nanoparticles on the surface of GR nanosheets, the nanocomposites show good biocompatibility with porous nanostructure and prevent the aggregation of the GR nanosheets. Shan et al. achieved a glucose biosensor based on immobilization of glucose oxidase in thin films of chitosan containing GR and gold nanoparticles [14]. Baby et al. fabricated metal decorated GR nanosheets for amperometric glucose sensor [15]. Guo et

* Corresponding author at: College of Chemistry and Chemical Engineering, Hainan Normal University, Haikou 571158, PR China. Tel./fax: +86 898 31381637.
E-mail address: swyy26@hotmail.com (W. Sun).

0928-4931/$ – see front matter © 2012 Elsevier B.V. All rights reserved.
http://dx.doi.org/10.1016/j.msec.2012.12.077

al. developed a one-pot rapid synthesis method to assemble Pt nanoparticles on the GR nanosheets for electrochemical sensing [16]. Bong et al. utilized the GR nanosheets as the catalyst support of PtRu nanoparticles for the electrooxidation of methanol [17].

Nafion is a perfluorinated anionic polyelectrolyte with good film forming ability, high chemical stability and good biocompatibility, which has been widely used for the immobilization of biomacromolecules [18]. Carbon ionic liquid electrode (CILE), which is prepared by mixing carbon powder with ionic liquids (ILs), has been widely used in the electrochemical sensor in recent years. CILE has exhibited many advantages such as high ionic conductivity, wide electrochemical windows and excellent antifouling ability, so it can be used as the basal electrode for the further modification [19]. Safavi et al. [20] fabricated a glucose sensor based on nanoscale nickel hydroxide modified CILE. Sun et al. [21] fabricated an N-butylpyridinium hexafluorophasphate based CILE for the electrochemical detection of DNA.

In this paper a new protein film based electrochemical biosensor was prepared with Mb as a model redox protein. Due to the deep burying of the redox proteins in the protein structures, direct electron transfer of redox proteins with underlying electrode is different to be realized. So it is necessary to use different kinds of promoters or mediators to enhance the electron transfer rate and shorten the distances between the redox electroactive centers with the substrate electrode. Also the biocompatibility of the electrode interface is needed to be remained to retain the biological structure of redox proteins. Different types of modifiers such as biopolymers, nanoparticles, ILs and surfactants had been used in the electrode modification. Also various fabrication processes such as layer-by-layer assemble, covalent binding, direct casting, and adsorption etc. were used. In this work a GR–Pt nanocomposite was synthesized and used for the electrode modification with a simple direct casting method. GR has been used in the field of electrochemical sensor with the advantages such as high conductivity, large surface area and electrocatalytic activity. Due to poor dispersibility of GR nanosheets in the solvent, GR tends to be an irreversible agglomerate together with the *van der Waals* interaction and strong π–π stacking to give multilayer GR sheets or even restack to graphite, which limits its electrochemical application. By decorating metal nanoparticles on the surface of GR nanosheets, the restacking of GR nanosheets could be prevented with the increase of the surface area. Also noble metal nanoparticles such as gold and platinum exhibit better electrocatalytic activity in the electrochemical sensing. So the GR–Pt nanocomposite was introduced in the electrode modification, which cannot only accelerate the electron transfer rate but also provide a specific three-dimensional interface for the protein immobilization. Direct electron transfer of the immobilized Mb was investigated with Nafion, GR–Pt nanocomposite and CILE. Due to the specific effects of GR–Pt nanocomposite such as high conductivity and porous structure, the fabricated bioelectrode showed excellent electrochemical behavior. Direct electrochemistry between Mb molecules and the substrate electrode was easily achieved. The results indicated that Nafion/GR–Pt nanocomposite could be a good candidate material for immobilizing biomolecules and fabricating the third-generation biosensors.

2. Experimental

2.1. Reagents and apparatus

1-Butylpyridinium hexafluorophosphate ($BPPF_6$, Lanzhou Greenchem ILS. LICP. CAS., China), horseheart myoglobin (Mb, MW 17800, Sigma), Nafion (5% ethanol solution, Sigma), graphite powder (average particle size 30 μm, Shanghai Colloid Chemical Company, China) and trichloroacetic acid (TCA, Tianjin Kemiou Chemical Limited Company) were used as received. 0.1 mol/L phosphate buffer solutions (PBS) with pH 7.0 were used as the supporting electrolyte. The GR–Pt nanocomposites were prepared according to the reference [22]. All the other chemicals used were of analytical reagent grade and the deionized water was used for all aqueous solutions.

A CHI 750B electrochemical workstation (Shanghai CH Instrument, China) was used for the electrochemical measurements. A conventional three-electrode system was used with a composite film modified electrode as working electrode, a platinum wire as auxiliary electrode and a saturated calomel electrode (SCE) as reference electrode. Ultraviolet-visible (UV-Vis) absorption spectra and Fourier transform infrared (FT-IR) spectra were recorded on a Cary 50 probe spectrophotometer (Varian Company, Australia) and a Tensor 27 FT-IR spectrophotometer (Bruker Company, Germany), respectively. Scanning electron microscopy (SEM) and transmission electron microscopy (TEM) were performed on JSM-6700F scanning electron microscope (Japan Electron Company, Japan) and JEOL JEM-2010HT transmission electron microscope (Japan Electron Company, Japan), respectively. Atomic force microscope (AFM) images were recorded on Benyuan CSPM-5000 scanning probe microscope (Benyuan Co., China) with a tapping mode. X-ray powder diffraction (XRD) pattern was operated on a Japan RigakuD/Maxr-A X-ray diffractometer equipped with graphite monochromatized high-intensity Cu·Kα radiation (λ = 1.54178 Å).

2.2. Synthesis of the GR–Pt nanocomposite

Graphite oxide (GO) was synthesized by the modified Hummer's method [23]. To obtain the Pt nanoparticles decorated GR nanosheets (GR–Pt), 51.0 mg GO was dissolved in 240 mL water by ultrasonic treatment for 1 h to form a homogenous suspension, and 10.0 mL 0.02 mol/L H_2PtCl_6 was added under stirring. The pH value of this mixture was adjusted to 11.86 by 1.0 mol/L NaOH. Then 2.0 g $NaBH_4$ was slowly added to the mixture with stirring for 26 h under room temperature. Finally, the solid sample with about 50% (wt.) Pt loading was collected after thorough washing with ethanol and deionized water, and vacuum-dried at 40 °C. Based on these procedures the pure GR–Pt nanocomposites could be prepared.

2.3. Fabrication of the Nafion/Mb–GR–Pt/CILE

CILE was fabricated by hand-mixing 0.50 g of $BPPF_6$ and 1.5 g of graphite powder in a mortar thoroughly. A portion of resulting homogeneous paste was packed firmly into a glass tube (Φ = 4 mm) and the electrical contact was established through a copper wire to the end of the paste in the inner hole of the tube. Prior to use a mirror-like surface was obtained by polishing the CILE surface on a weighing paper.

The modifier was prepared by mixing 10.0 mg Mb and 9.0 μL 1.0 mg/mL GR–Pt dispersion solution into 1.0 mL 0.1 mol/L PBS (pH = 7.0) with oscillating for 1 min. Then 8.0 μL of the prepared mixture was dropped on the surface of CILE and left it to dry at room temperature. Finally, 8.0 μL of 0.5% Nafion was cast on electrode surface to form a stable film. The resulted electrode was denoted as Nafion/Mb–GR–Pt/CILE. Other modified electrode such as Nafion/Mb/CILE was prepared by similar procedure and used for comparison. All the electrodes were stored at 4 °C in a refrigerator under dry conditions when not in use.

2.4. Procedure

Electrochemical experiments were carried out in a 10 mL electrochemical cell containing 0.1 mol/L PBS, which was purged with highly purified nitrogen for 30 min prior to the experiments and a nitrogen environment was kept during the electrochemical measurements. The Nafion/Mb–GR–Pt film assembled on a glass slide was used for FT–IR measurements. UV-Vis spectroscopic experiments were performed with a mixture solution of Mb, Nafion, GR–Pt with pH 7.0 PBS and scanned in the wavelength range from 320 to 550 nm.

3. Results and discussion

3.1. Characterization of nanocomposite

The synthesized nanomaterials were first characterized by SEM. As shown in Fig. 1A, the morphology of GO exhibited a typical irregular sheet shape with a three-dimensional structure, which was suitable for the further decoration with metal nanoparticles. The SEM morphology of as-synthesized GR–Pt material was shown in Fig. 1B with the enlarged image exhibited as the inset of Fig. 1B. It was obvious that the individual Pt nanoparticles were well-separated from each other and well-spread out on the surface of GR sheets with an average diameter of 60 nm. The morphology of GR–Pt nanocomposite was further characterized by TEM with the results shown in Fig. 1C. It can be seen that the individual Pt nanoparticles were well-spread and decorated on the GR sheets, which appeared as many dark dots dispersed uniformly on the lighter GR sheets. The results can be further proved by the enlarged TEM image (inset of Fig. 1C) with many small nanoparticles formed on the GR surface with better homogeneous distribution. The appearances of some large particles may be attributed to the fold of GR nanosheets with the overlapped of the small particles to large ones. Typical AFM image of GR–Pt nanocomposite was further recorded with the results shown in Fig. S1A. It can be seen that Pt nanoparticles were decorated on the surface of GR sheets and the average thickness of GR sheets was calculated as 4.5 nm by the cross section analysis (as shown in Fig. S1B). However, single-sheet GR is typically found to be in the order of 0.9–1.3 nm when analyzed by AFM. The results indicated that a multilayer of GR was formed due to the fluctuated and bended appearance of single layer of GR. Fig. 1D showed the X-ray powder diffraction (XRD) pattern of the final product. The obvious peaks appeared on the XRD results with the (111), (200) and (220) diffraction peaks of Pt (JCPDS card, no. 87-0647), indicating that Pt nanoparticles were present in a crystalline state. All the above results indicated that a GR–Pt nanocomposite was successfully synthesized.

3.2. Spectroscopic result

UV-Vis absorption spectroscopy is a useful conformational probe to investigate the second structure of redox proteins. In UV-Vis absorption spectrum the Soret band from the four iron heme groups of heme proteins may provide the information on the conformational integrity of the proteins and the possible denaturation or the conformational change about the heme region [3]. As shown in Fig. 2 A, the Soret band of Mb appeared at 407.0 nm in 0.1 mol/L pH 7.0 PBS (curve a). While the mixture of Mb with Nafion and GR–Pt in PBS exhibited the same Soret band with that of Mb solution, which indicated that Mb in the composite matrix retained its native structure.

FT-IR spectroscopy is also used to check the conformational integrity of the heme proteins. The shape and position of the amide I and II infrared absorbance bands of proteins can provide information on the secondary structure of the polypeptide chain. The amide I band (1700–1600 cm^{-1}) is attributed to the C═O stretching vibration of the peptide linkage in the backbone of protein. The amide II band (1600–1500 cm^{-1}) is caused by the combination of N–H inplane bending and C–N stretching vibration of the peptide groups [24]. If the protein molecule is denatured, the intensities and shape of the amide I and II bands will diminish or even disappear [25,26]. As shown in Fig. 2 B, the amide I and II bands of Mb in Nafion–GR–Pt composite film appeared at 1642 cm^{-1} and 1537 cm^{-1} (Fig. 2B b),

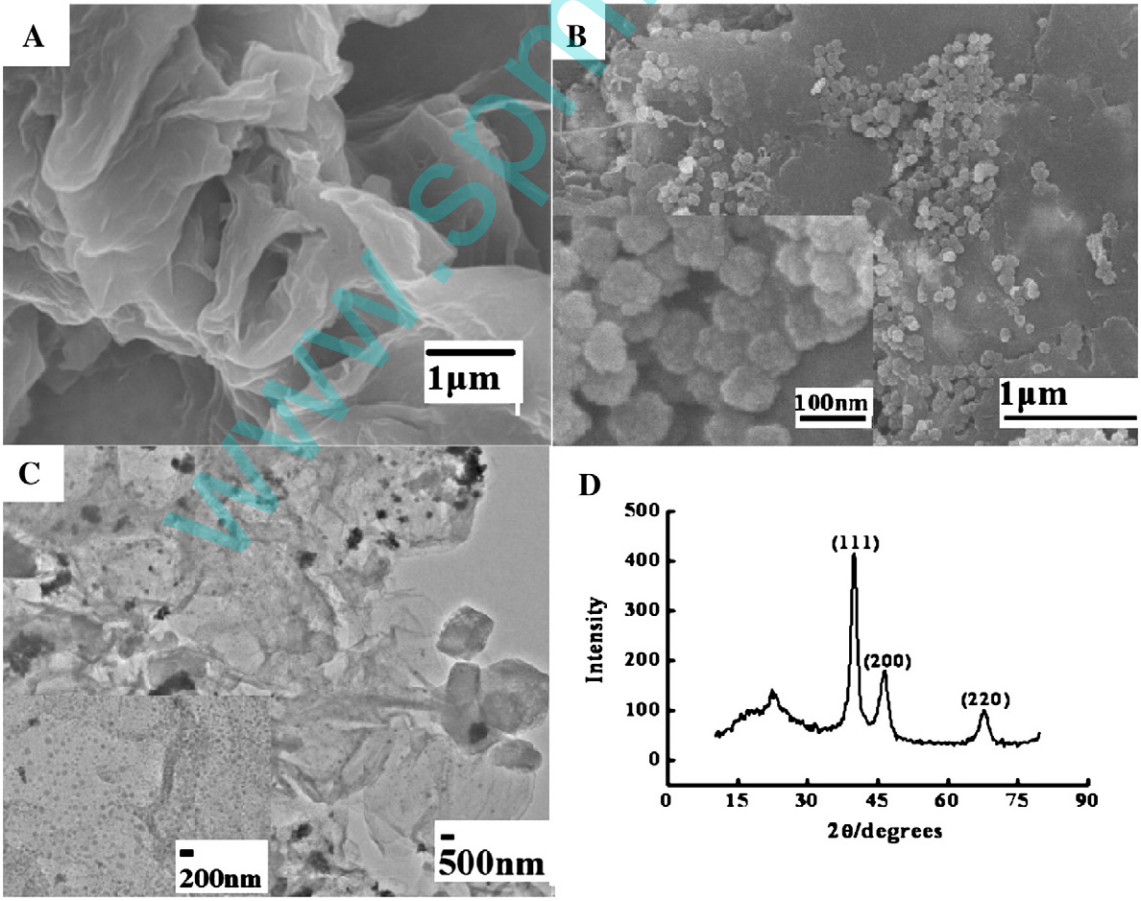

Fig. 1. SEM images of GO sheet (A) and GR–Pt nanocomposite (B) with inset as the enlarged of image; (C) TEM image of GR–Pt nanocomposite with inset as the enlarged image; and (D) XRD result of GR–Pt nanocomposite.

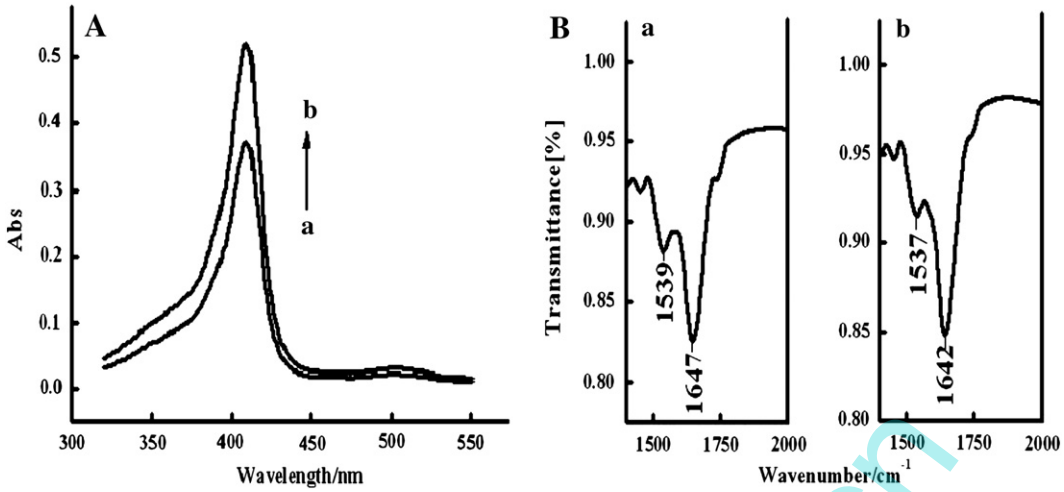

Fig. 2. (A) UV-Vis absorption spectra of Mb (a) and Nafion–GR–Pt–Mb mixture (b) with pH 7.0 PBS, (B) FT-IR spectra of (a) Mb and (b) Nafion/GR–Pt–Mb film.

which had the similar position to the native state of Mb at 1647 cm^{-1} and 1539 cm^{-1} (Fig. 2B a). The results also indicated that the native structure of Mb was not changed in the Nafion–GR–Pt film.

3.3. Electrochemical impedance spectroscopy of the modified electrode

Electrochemical impedance spectroscopy (EIS) can give information on the impedance changes of the interface during the modification process. The semicircular portion at high frequencies in the Nyquist diagrams corresponds to the electron-transfer-limited process and its diameter is equal to the electron-transfer resistance (Ret), which controls the electron-transfer kinetics of the redox probe at the electrode. Meanwhile, the linear part at lower frequencies corresponds to the diffusion process. Fig. 3 exhibited the EIS results of different modified electrodes in the presence of 5.0 mmol/L $K_3[Fe(CN)_6]/K_4[Fe(CN)_6]$ and 0.1 mol/L KCl mixture solution with the frequency swept from 10^4 to 0.1 Hz. The AC voltage amplitude was set as 5 mV and the applied potential was 202 mV. The Ret value of bare CILE was got as 89 Ω (curve a), indicating that the charge transfer at bare electrode was relatively facile. When Nafion and Mb were coated on the electrode, a substantial increase in the diameter of the semicircle was observed with the Ret value as 167 Ω (curve b). The reason was due to the presence of Nafion and Mb molecules on the electrode surface could act as the inert electron and mass transfer blocking layer, and hinder the diffusion of ferricyanide toward the electrode surface. When GR–Pt nanocomposite was added on the electrode surface, the diameter of Nyquist circle decreased dramatically with the Ret value as 34 Ω (curve c). Because GR–Pt nanocomposite has good conductivity with large surface area, the presence of GR–Pt nanocomposite on the electrode surface can act as a good electron–transfer media between the probe and the electrode, which accelerate the electron transfer rate of the $[Fe(CN)_6]^{3-/4-}$ redox probe.

3.4. Electrochemical characteristics of Nafion/Mb–GR–Pt/CILE

Direct electrochemical behaviors of different modified electrodes were carefully investigated in pH 7.0 PBS by cyclic voltammetry with the results showed in Fig. 4. No electrochemical responses were observed at Nafion/CILE (curve a), indicating no electroactive substances existed on the electrode surface. After the addition of Mb on the electrode surface, a pair of small and unsymmetric redox peaks appeared (curve b), indicating that direct electron transfer between Mb and CILE was partly realized. Mb is a heme protein with electroactive center, which can exchange the electron with the substrate electrode under certain condition. CILE is a kind of modified electrode with high conductivity and biocompatible interface, which is suitable for the protein immobilization [27]. The small redox peaks of Nafion/Mb/CILE indicated that the electron transfer rate was slow. After the addition of GR–Pt nanocomposite in the Mb modified electrode, the redox peak currents increased gradually than that of Nafion/Mb/CILE with the peak shape more symmetry (curve c). Also the redox peaks almost unchanged after continuous potential cycling. The results indicated that direct electron transfer rate of Mb was enhanced on GR–Pt modified electrode with good stability. So

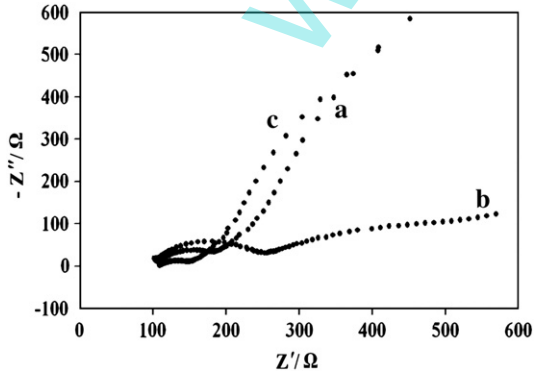

Fig. 3. Electrochemical impedance spectroscopy of (a) CILE, (b) Nafion/Mb/CILE, and (c) Nafion/Mb–GR–Pt/CILE in the presence of a solution of 5.0 mmol/L $[Fe(CN)_6]^{3-/4-}$ and 0.1 mol/L KCl with the frequencies from 10^4 to 0.1 Hz.

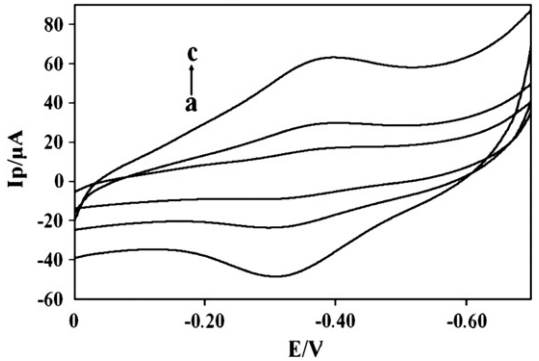

Fig. 4. Cyclic voltammograms of (a) CILE, (b) Nafion/Mb/CILE and (c) Nafion/Mb–GR–Pt/CILE in pH 7.0 PBS at the scan rate of 100 mV/s.

the presence of high conductive GR–Pt nanocomposite played an important role in establishing a fast electron transfer path to facilitate the direct electrochemistry of Mb with the underlying electrode. When Pt nanoparticles were decorated on the GR nanosheets, an increase of the surface area and surface roughness could be resulted. Also the GR–Pt nanocomposite combined the good conductivity and electrocatalytic ability of GR and Pt together, which was a benefit for the acceleration of electron transfer between the Mb active centers with electrode. From curve c the values of anodic peak potential (E_{pa}) and cathodic peak potential (E_{pc}) were derived at −0.311 V and −0.394 V, respectively. The formal peak potential ($E^{0'}$), which is calculated from the midpoint of E_{pa} and E_{pc}, was estimated as –0.352 V (vs. SCE). The result was the typical characteristic of electroactive heme Fe(III)/Fe(II) redox couples. So the direct electron transfer of Mb was successfully realized on the GR–Pt nanocomposite film modified electrode.

The influence of scan rate on the electrochemical responses of Nafion/Mb–GR–Pt/ CILE was further investigated by cyclic voltammetry with the results shown in Fig. 5. It can be seen that a pair of symmetric redox peaks appeared in the scan rate range from 50 to 600 mV s^{-1}. The redox peak currents increased gradually with the increase of scan rate and the relationships were established with two linear regression equations as $I_{pc}(\mu A) = 56.64\,\upsilon$ (V/s)–1.60 ($\gamma = 0.997$) and $I_{pa}(\mu A) = -52.78\,\upsilon$ (V/s)–4.02 ($\gamma = 0.998$), respectively. The results indicated that the electrochemical behavior of Mb immobilized on the modified electrode was a surface-controlled thin-layer process, in which the electroactive Mb·Fe(III) in the film were reduced to Mb·Fe(II) on the forward cyclic voltammetric scan and then fully reoxidized to Fe(III) on the reversed scan.

With the increase of scan rate, the peak-to-peak separation (ΔE_p) also increased gradually, which indicated a quasi-reversible electrochemical process. Then the electrochemical parameters were calculated according to the model of Laviron's equations [28]:

$$Epc = E^{0'} - \frac{2.3RT}{\alpha nF}\log \upsilon \quad (1)$$

$$Epa = E^{0'} + \frac{2.3RT}{(1-\alpha)nF}\log \upsilon \quad (2)$$

$$\log k_s = \alpha\log(1-\alpha) + (1-\alpha)log\alpha - \log\frac{RT}{nFv} - \frac{(1-\alpha)\alpha Fn\Delta Ep}{2.3RT} \quad (3)$$

where α is the electron transfer coefficient, k_s is the apparent heterogeneous electron transfer rate constant, R is the gas constant and T is the absolute temperature. Two straight lines were derived from the equations as $E_{pa}(V) = 0.0108\ \ln\nu - 0.308$ ($\gamma = 0.996$) and $E_{pc}(V) = -0.0311\ \ln\nu - 0.391$ ($\gamma = 0.997$). Then the values of α and k_s were calculated as 0.472 and 0.584 s^{-1}, respectively. It is well-known that k_s reflects the local microenvironment of the protein immobilized on the electrode and the value obtained here is in the range of k_s for typical surface-controlled quasi-reversible electron transfer processes. This k_s value is higher than that of Mb immobilized on Ag-CNTs/GCE (0.41 s^{-1}) [29] and Nafion/MWCNTs/CILE (0.33 s^{-1}) [30], so the electron transfer of Mb was facile due to the specific microenvironment provided by Nafion/GR–Pt composite film.

From the integration of the cyclic voltammetric reduction peaks, the surface concentration (Γ^*) of electroactive Mb in the composite can be calculated from the equation: $Q = nFA\Gamma^*$ [31], where Q is the charge passing through the electrode with full reduction of electroactive Mb, n is the number of electron transferred, F is the Faraday's constant, A is the area of electrode. The value of Γ^* was 4.43×10^{-8} mol/cm^2, which was much greater than the theoretical monolayer coverage of 1.89×10^{-11} mol/cm^2 [32]. The total amount of Mb cast on the electrode surface was calculated as 7.65×10^{-8} mol/cm^2, so 57.9% of the immobilized Mb took part in the electrochemical reaction. The result also demonstrated that the composite film provided a specific three-dimensional porous microstructure with higher conductivity, which was a benefit for multilayers of Mb on the electrode to exchange electrons with the basal electrode.

3.5. Effect of pH

The solution pH can strongly affect the electrochemical behaviors of redox protein on the electrode surface. So the influence of buffer pH on the electrochemical responses of Nafion/Mb–GR–Pt/CILE was investigated with the results shown in Fig. 6. In each pH solution a pair of stable and well-defined reversible redox peaks of Mb was observed. Furthermore both anodic and cathodic peak potentials were shifted to the negative direction with the increase of pH value from 4.0 to 10.0, and the maximum current response was occurred at pH 7.0. In addition the formal peak potential ($E^{0'}$) had a linear relationship with pH from 5.0 to 8.5 with a slope value of −44.6 mV/pH (shown as inset of Fig. 6), which was reasonably close to the theoretical value of −59 mV/pH. This may be owing to the effects of the protonation states of transligands to the heme iron and amino acids around the heme to the protonation of water molecules coordinated to the center, which may exist in different states under different pH values [33]. Thus, the electron-transfer between Mb and the electrode can be presented by the following equation: Mb Fe(III) + H^+ + e^- ⇌ Mb Fe(II).

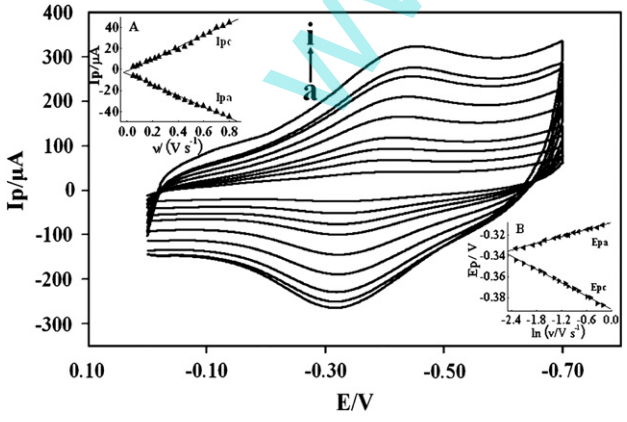

Fig. 5. Cyclic voltammograms of Nafion/Mb–GR–Pt/CILE in pH 7.0 PBS with different scan rates (from a to i are 50, 100, 150, 200, 300, 400, 500, 550, and 600 mV/s, respectively). Inset A: Linear relationship of cathodic and anodic peak current (I_p) versus scan rate (υ); Inset B: Linear relationship of the redox peak potential E_{pa} and E_{pc} versus lnυ.

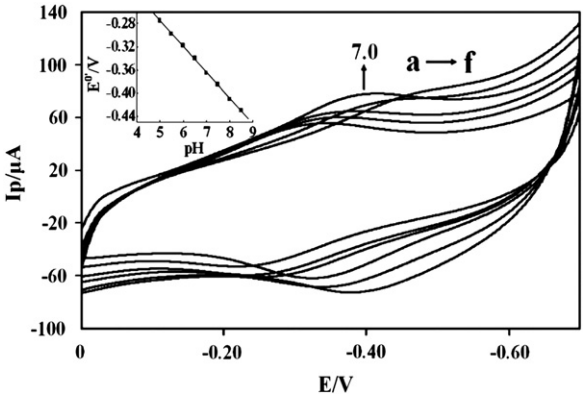

Fig. 6. Cyclic voltammograms of Nafion/Mb–GR–Pt/CILE in 0.1 mol/L PBS at different pH values (from a to f: 5.0, 5.5, 6.0, 7.0, 7.5, 8.5) with the scan rate as 100 mV/s. Inset: relationship of the formal peak potential ($E^{0'}$) with pH.

3.6. Electrocatalytic activity

TCA is an analog of acetic acid in which three hydrogen atoms of the methyl group have all been replaced by chlorine atoms. It is widely used in biochemistry for the precipitation of macromolecules such as proteins, DNA and RNA, and cosmetic treatments such as chemical peels and tattoo removal. The bioelectrocatalytic behavior of the Mb modified electrode towards TCA was further explored by cyclic voltammetry with the results shown in Fig. 7. Upon the addition of TCA to 0.1 mol/L PBS (pH 7.0), cyclic voltammograms of Nafion/Mb–GR–Pt/CILE changed dramatically with an increase of reduction peak current at −0.526 V and a decrease of oxidation peak current (curves c–o), demonstrating a typical electrocatalytic reduction. While no redox peak was observed at Nafion/GR–Pt/CILE under the same conditions without Mb in the composite film (curves a and b). According to the reference [34], the reaction processes were proposed as follows:

$$\mathrm{Mb\,Fe(III)} + \mathrm{e} \rightleftharpoons \mathrm{Mb\,Fe(II)} \quad \text{at electrode}$$

$$\mathrm{Cl_3CCOOH} \rightleftharpoons \mathrm{Cl_3CCOO^-} + \mathrm{H^+} \quad p\mathit{K}a = 0.89$$

$$2\,\mathrm{Mb\,Fe(II)} + \mathrm{Cl_3CCOOH} + \mathrm{H^+} \rightarrow 2\,\mathrm{Mb\,Fe(III)} + \mathrm{Cl_2HCCOOH} + \mathrm{Cl^-}.$$

The catalytic reduction peak currents increased with the TCA concentration in the range from 0.9 to 9.0 mmol/L with the linear regression equation as I_{pc} (μA) = 30.08 C (mmol/L)–36.34 (γ = 0.997) and the detection limit as 0.32 mmol/L (3σ). The detection limit for TCA detection was smaller than that of the $\{PDDA/Hb\}_8$ films modified pyrolytic graphite electrode (PGE) (1.98 mmol/L) [35], $\{(PS–Hb)/PSS\}_6$ modified PGE (3.0 mmol/L) [36] and Nafion/nano-CdS/Hb/CILE (10.0 mmol/L) [37], indicating the better performance of the GR–Pt nanocomposite modified electrode. When the TCA concentration was more than 9.0 mmol/L, the reduction peak current turned to level off, indicating a typical Michaelis–Menten kinetic process. So the apparent Michaelis–Menten constant (K_M^{app}) was calculated to be 0.126 mmol/L according to the Lineweaver–Burk equation [38]. Compared with other kinds of Mb modified electrodes, this K_M^{app} value is lower than the report values such as that of Nafion/Mb/MWCNTs/CILE (1.227 mmol/L) [30] and Mb-DNA-CILE (0.820 mmol/L) [39], which indicated that Mb immobilized in Nafion/GR–Pt/CILE retained its bioactivity and had a high biological affinity to TCA.

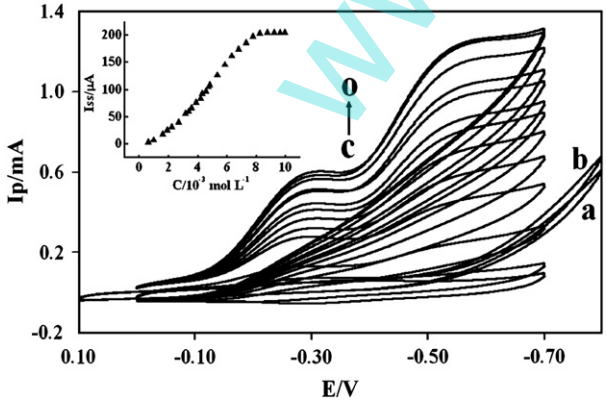

Fig. 7. Cyclic voltammograms of Nafion/GR–Pt/CILE in the presence of (a) 0, (b) 10.0 mmol/L TCA in 0.1 mol/L pH 7.0 PBS and Nafion/Mb–GR–Pt/CILE in the presence of 0, 2.0, 2.5, 3.5, 4.5, 5.0, 5.5, 6.0, 7.0, 8.0, 8.5, 10.0, and 12.0 mmol/L TCA (curves c to o) with the scan rate as 100 mV/s. Inset was the linear relationship of catalytic reduction peak currents and the TCA concentration.

3.7. Stability and reproducibility of Nafion/Mb–GR–Pt/CILE

The storage stability of Nafion/Mb–GR–Pt/CILE was investigated by storing it at 4 °C and measured intermittently. Ten days later the response of the modified electrode retained 94.3% of its initial value. After 1 month of testing, the peak current response decreased about 9.5%. The reproducibility of the current response for Nafion/Mb–GR–Pt/CILE was examined with a 3.0 mmol/L TCA solution and the relative standard deviation (RSD) was calculated as 3.5% for 10 independent determinations. The above results indicated the good stability and reproducibility of the modified electrode. Ten Mb modified electrodes were prepared by the same procedure independently and the RSD value for the determination of 3.0 mmol/L TCA was calculated as 4.5%, which indicated the modified electrode had good repeatability.

4. Conclusions

In this paper a GR–Pt nanocomposite was synthesized and further employed for the immobilization of Mb molecules on CILE surface with a Nafion film. UV-Vis absorption and FT-IR spectra indicated that Mb retained its native structure in the Nafion–GR–Pt nanocomposite. The utility of high conductive GR–Pt nanocomposite with big surface area can endow the immobilized Mb molecules with well-maintained bioactivity and enhanced transfer rate. A pair of well-defined redox peaks appeared on the cyclic voltammograms, which indicated that the direct electrochemistry of Mb was realized. The prepared biosensor exhibited excellent electrochemical response to the reduction of TCA without the addition of the electron mediators. So the strategy indicated that GR–Pt nanocomposite modified electrode could serve as a good electrochemical sensing platform for other bioactive molecules in various biosensor designs.

Supplementary data to this article can be found online at http://dx.doi.org/10.1016/j.msec.2012.12.077.

Acknowledgments

We acknowledge the financial support provided by the National Natural Science Foundation of China (21075071), the Nature Science Foundation of Hainan Province (212013), the Doctoral Foundation of QUST (0022424) and the Foundation of Hainan Normal University.

References

[1] F.A. Armstrong, H.A.O. Hill, N.J. Walton, Acc. Chem. Res. 21 (1988) 407–413.
[2] F.W. Scheller, N. Bistolas, S.Q. Liu, M. Janchem, M. Katterle, U. Wollenberger, Adv. Colloid Interface Sci. 116 (2005) 111–120.
[3] J.F. Rusling, A.E.F. Nassar, J. Am. Chem. Soc. 115 (1993) 11891–11897.
[4] P. Bianco, Mol. Biotechnol. 82 (2002) 393–409.
[5] S.F. Ding, M.Q. Xu, G.C. Zhao, X.W. Wei, Electrochem. Commun. 9 (2007) 216–220.
[6] L. Ma, Y.N. Tian, Z.J. Rong, J. Biochem. Biophys. Methods 70 (2007) 657–662.
[7] W. Sun, X.Q. Li, P. Qin, K. Jiao, J. Phys. Chem. C 113 (2009) 11294–11300.
[8] X. Huang, X.Y. Qi, F. Boey, H. Zhang, Chem. Soc. Rev. 41 (2012) 666–686.
[9] X.L. Li, X.R. Wang, L. Zhang, S. Lee, H.J. Dai, Science 319 (2008) 1229–1232.
[10] V. Singh, D. Joung, L. Zhai, S. Das, S.I. Khondaker, S. Seal, Prog. Mater. Sci. 56 (2011) 1178–1271.
[11] M.J. Allen, V.C. Tung, R.B. Kaner, Chem. Rev. 110 (2010) 132–145.
[12] S. Stankovich, D.A. Dikin, G.H.B. Dommett, K.M. Kohlhaas, E.J. Zimney, E.A. Stach, R.D. Piner, S.T. Nguyen, R.S. Ruoff, Nature 442 (2006) 282–286.
[13] N.O. Weiss, H.L. Zhou, L. Liao, Y. Liu, S. Jiang, Y. Huang, X.F. Duan, Adv. Mater. 43 (2012) 5782–5785, http://dx.doi.org/10.1002/adma.201201482.
[14] C.S. Shan, H.F. Yang, D.X. Han, Q.X. Zhang, A. Ivaska, L. Niu, Biosens. Bioelectron. 25 (2010) 1070–1074.
[15] T.T. Baby, S.S. Aravind, T. Arockiadoss, R.B. Rakhi, S. Ramaprabhu, Sens. Actuators B: Chem. 145 (2010) 71–77.
[16] S.J. Guo, D. Wen, Y.M. Zhai, S.J. Dong, E.K. Wang, ACS Nano 4 (2010) 3959–3968.
[17] S.Y. Bong, Y.R. Kim, I. Kim, S.H. Woo, S.Y. Uhm, J.Y. Lee, H. Kim, Electrochem. Commun. 12 (2010) 129.
[18] W.W. Yang, Y.C. Li, Y. Bai, C.Q. Sun, Sens. Actuators B 115 (2006) 42–48.
[19] M.J.A. Shiddiky, A.A.J. Torriero, Biosens. Bioelectron. 26 (2011) 1775–1787.
[20] A. Safavi, N. Maleki, E. Farjami, Biosens. Bioelectron. 24 (2009) 1655–1660.
[21] W. Sun, Y.Z. Li, M.X. Yang, S.F. Liu, K. Jiao, Electrochem. Commun. 10 (2008) 298–301.
[22] Y.M. Li, L.H. Tang, J.H. Li, Electrochem. Commun. 11 (2009) 846–849.

[23] W.S. Hummers, R.E. Offeman, J. Am. Chem. Soc. 80 (1958) 1339.
[24] J.K. Kauppinen, D.J. Moffatt, H.H. Mantsch, D.G. Cameron, Appl. Spectrosc. 35 (1982) 271–276.
[25] Y.P. Song, M.C. Petty, J. Yarwood, W.J. Feast, J. Tsibouklis, S. Mukherjee, Langmuir 8 (1992) 257–261.
[26] A.E. Nassar, W.S. Willis, J.F. Rusling, Anal. Chem. 67 (1995) 2386–2392.
[27] W. Sun, D.D. Wang, R.F. Gao, K. Jiao, Electrochem. Commun. 9 (2007) 1159–1164.
[28] E. Laviron, J. Electroanal. Chem. 101 (1979) 19–28.
[29] C.Y. Liu, J.M. Hu, Biosens. Bioelectron. 24 (2009) 2149–2154.
[30] W. Sun, X.Q. Li, Y. Wang, X. Li, C.Z. Zhao, K. Jiao, Bioelectrochemistry 75 (2009) 170–175.
[31] A.J. Bard, L.R. Faulkner, Electrochemical methods, fundamentals and applications, Wiley, New York, 1980, p. 525.
[32] S.F. Wang, T. Chen, Z.L. Zhang, D.W. Pang, K.Y. Wong, Electrochem. Commun. 9 (2007) 1709–1714.
[33] I. Yamazaki, T. Araiso, Y. Hayashi, Y. Yamada, R. Makino, Adv. Biophys. 11 (1978) 249–281.
[34] C.H. Fan, Y. Zhuang, G.X. Li, J.Q. Zhu, D.X. Zhu, Electroanalysis 12 (2000) 1156–1158.
[35] P.L. He, N.F. Hu, G. Zhou, Biomacromolecules 3 (2002) 139–146.
[36] H. Sun, N.F. Hu, Analyst 130 (2005) 76–84.
[37] W. Sun, D.D. Wang, G.C. Li, Z.Q. Zhai, R.J. Zhao, K. Jiao, Electrochim. Acta 53 (2008) 8217.
[38] R.A. Kamin, G.S. Wilson, Anal. Chem. 1980 (52) (1980) 1198–1205.
[39] R.F. Gao, J.B. Zheng, Electrochem. Commun. 11 (2009) 1527–1529.